



Albedo of summer snow on sea ice, Ross Sea, Antarctica

Xiaobing Zhou,¹ Shusun Li,² Kim Morris,² and Martin O. Jeffries²

Received 10 August 2006; revised 8 March 2007; accepted 9 May 2007; published 22 August 2007.

[1] Surface all-wave albedo and physical parameters (grain radius, mass density, surface temperature, and stratification) of an austral summer snow cover on sea ice were measured in the Ross Sea during January-February 1999. It was observed that (1) from north to south the snow surface temperature decreases, albedo increases, snow mass density decreases, snow composite grain radius decreases, and number density of composite grains increases; (2) the size of the clusters of snow grains (i.e., melt clusters and well-bonded chains of grains), rather than the size of the individual snow grains, is the dominant parameter controlling albedo (the smaller the snow composite grain radius and the larger the number density are, the higher the albedo is); and (3) in determining the snow albedo, grain size dominates over the number density and the upper layers dominate over the lower layers. A comparison of the statistical relation between albedo and the averaged grain size shows that statistical significance is independent of the selection of the grain size averaging method. Suggestions for snow albedo parameterization are made.

Citation: Zhou, X., S. Li, K. Morris, and M. O. Jeffries (2007), Albedo of summer snow on sea ice, Ross Sea, Antarctica, *J. Geophys. Res.*, 112, D16105, doi:10.1029/2006JD007907.

1. Introduction

[2] All-wave albedo (hereafter called albedo) is defined as the ratio of the reflected solar irradiance (W/m^2) to the incident irradiance of the whole solar spectrum at the Earth surface. Albedo determines how much shortwave solar energy is absorbed by the earth surface, which in turn drives the geophysical, oceanographic, biogeochemical, ecological, climatological, and hydrological activities on earth. The albedo of snow and ice surfaces has a positive feedback with snowpack temperature change. An increase in temperature may result in a decrease in the albedo of the snow and ice; in turn, solar energy absorption increases, and eventually may result in the melting of the snow and ice cover and a further increase in temperature as a lower albedo surface (land or water) is exposed. This positive feedback of snow and ice albedo will amplify the temperature change due to greenhouse gas warming in the polar regions [Houghton *et al.*, 1990, 1992]. Snow and ice albedo is thus an important parameter in the energy balance in either small-scale mass balance models [Schramm *et al.*, 1997] or large-scale land surface models (LSMs) and general circulation models (GCMs) [Desborough and Pitman, 1998; Marshall *et al.*, 1999; Yang and Niu, 2003; Takata *et al.*, 2003]. Therefore accurate specification of snow albedo is imperative in the modeling of land-surface-atmosphere interaction. Although there is increasing interest in assimilating the remotely sensed land surface albedo into climate models, at present

more effort is still needed on the parameterization of snow albedo [Bonan *et al.*, 2002; Dai *et al.*, 2003]. A physically accurate parameterization of albedo must be included in climate modeling so that the effect of the positive feedback of albedo can be properly addressed [Curry *et al.*, 2001]. Development of such parameterization schemes should eventually lead to the correct selection of albedo-controlling parameters and albedo parameterization schemes based on radiative transfer modeling and/or the establishment of a comprehensive geodatabase of snow albedo values from field measurements and satellite remote sensing [Schaaf *et al.*, 2002]. Satellite-derived albedo can offer improved estimates of surface albedo as compared to parameterizations or the limited spatial and/or temporal coverage of field measurements.

[3] Snow albedo is an important parameter but is very difficult to determine as it is affected by conditions of snow, atmosphere, and surface topography [Wiscombe and Warren, 1980; Warren and Wiscombe, 1980; Zhou *et al.*, 2003a]. Under given sky and surface physical conditions, albedo is easy to measure on the ground but harder to estimate from space and is theoretically difficult to quantify. From the viewpoint of scattering theory, particles (scatterers) in a light-scattering layer are characterized by their number density, shape, orientation, size, structure (uniform or nonuniform), and chemical composition [Bohren and Huffman, 1983; Zhou *et al.*, 2003b; Li and Zhou, 2004]. For snow cover, if the particles are optically represented as spheres, spectral albedo of snow will be determined mainly by the snow grain size, number density, thickness, impurity, and stratigraphy within the light-absorbing/scattering layer. On the basis of the radiative transfer modeling, the spectral albedo of snow is independent of snow density when the snowpack reaches semi-infinite depths. In addition, all-wave albedo

¹Department of Geophysical Engineering, Montana Tech of the University of Montana, Butte, Montana, USA.

²Geophysical Institute, University of Alaska, Fairbanks, Alaska, USA.

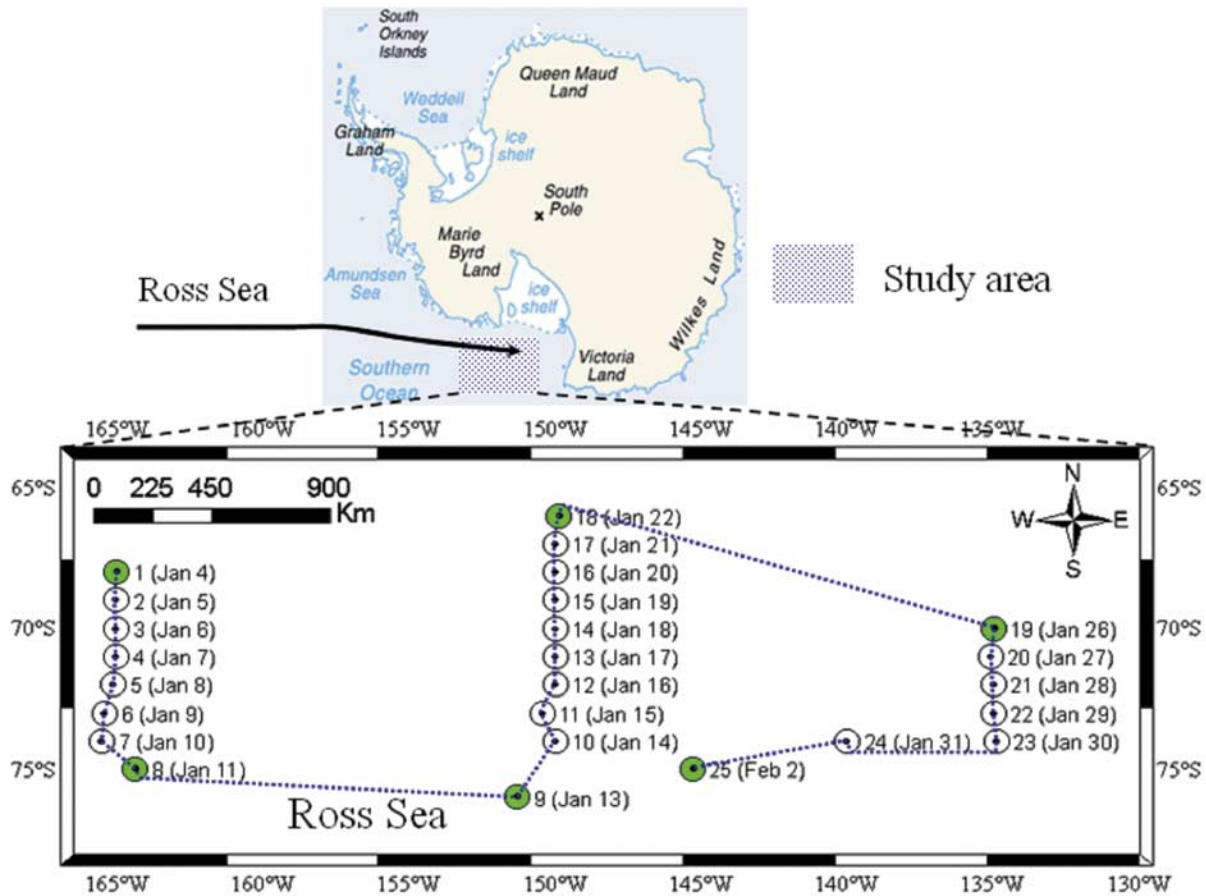


Figure 1. Route of R/V *Nathaniel B. Palmer* during a summer cruise in the Ross Sea, Antarctica (January and February 1999). Ice stations where albedo and snow pit work were carried out are indicated by a number with dates in parentheses. The open circles indicate the data sets used in this analysis, and the solid circles are the stations at ice edge.

also depends on geometrical and spectral characteristics of the incident radiation. The spectral characteristics of the incident radiation depend on the spectral optical depth of atmospheric cloud and atmospheric composition because clouds and atmospheric composition alter the spectral distribution of the downwelling solar irradiance. Parameters affecting the incident radiation include solar zenith angle [Dirmhirn and Eaton, 1975; Warren, 1982], cloud type, thickness and distribution [Male and Granger, 1981; Warren, 1982], and atmospheric parameters such as precipitable water, aerosol, and ozone content.

[4] The objectives of this paper are (1) to investigate the spatial variability of albedo and snow physical parameters in the Ross Sea, where very few albedo measurements and physical analysis have ever been carried out [Massom *et al.*, 2001; Brandt *et al.*, 2005]; (2) to study the statistical relationship between snow albedo and snow physical properties using in situ data collected in the Ross Sea to provide some insights in snow albedo parameterization; (3) to assess the impact of the selection of snow grain size averaging models on the statistical analysis mentioned in (2); and (4) to provide some simple albedo parameterization

schemes for the austral summer snow cover on sea ice in the Ross Sea.

2. Study Area and Methods

2.1. Cruise Tracks and Field Methods

[5] The austral summer cruise on the *Nathaniel B. Palmer* occurred in January–February 1999 in the Ross Sea. Ice stations were set up from the northern edge to the southern edge of the pack ice along three lines of longitude: 135°W, 150°W and 165°W (Figure 1). The interval between any two ice stations along a transect was about one degree of latitude. Seven to ten ice stations were made along each line of almost constant longitude which provides the opportunity to investigate the latitudinal variation of albedo and snow physical parameters. Albedo and snow pit measurements were made at each station. Albedo was measured at a time interval of 20 s to 60 s for 2–4 hours along with a vertical profile of snow physical parameters obtained adjacent to the albedo measurement site.

[6] Albedo was measured with a pair of Eppley PSP broadband precision spectral pyranometers. The albedo value at each ice station is the averaged values over the

measuring period, which generally occurred at 1000 to 1400 local solar time. Thus the mean solar zenith angle for all sites is approximately the same. Consequently, the effect of solar zenith angle on the spatial variability of albedo is neglected in the following discussion. An Exergen Model D-501-RS Infrared Microscanner was used to collect the surface temperature data at the location where albedo data were collected so that the snow surface was not disturbed [Li *et al.*, 1999].

[7] A snow pit was dug in the vicinity of the albedo measurement site at each ice station. The stratigraphy of the snow cover was determined and a series of snow samples of 100 cm³ each were taken at 3 cm intervals, i.e., the height of the snow cutter, from the snow surface (0 cm) down to the underlying sea ice surface. Therefore, in the following discussion, each 3 cm depth is considered as a layer. Snow physical parameters (composite grain radius, single grain radius, mass density, and relative mass percentage of each particle type (clusters, facets, striates, etc.) with mean radius $\langle r \rangle$) in each layer were determined from these samples using the International Association of Scientific Hydrology (IASH) International Classification for Seasonal Snow on the Ground [Colbeck *et al.*, 1990; Morris and Jeffries, 2001]. Snow surface temperatures oscillated around 0°C during the research cruise, causing single snow grains to bond together and form clusters through the melt-freeze cycle (see section 3). Therefore, in the following discussion, a composite grain refers to a well-bonded cluster of snow grains (individual grains are still distinguishable) or multicrystalline melt-freeze grains. A single grain refers to an individual snow grain. The long and short axes of a subsample of grain from each snow density sample were measured under a microscope. In this context, the radius of a composite grain or a single grain refers simply to the arithmetic average of these two values. Details of snow pit data (method and results) have been described elsewhere [Morris and Jeffries, 2001].

[8] We face two options when simulating snow albedo using radiative transfer theory or investigating the relationship between albedo and snow physical parameters: treat snow as a disperse medium composed completely of single grains, ignoring the connectivity between grains, or treat it as a disperse medium of composite grains, taking the connectivity into account. In this paper, we will investigate statistically which option is more relevant to the relationship between albedo and snow physical parameters, observed on snow on sea ice in the Ross Sea of Antarctica.

2.2. Statistical Analysis Methods

[9] In a light-scattering layer, snow particles are characterized by means of their grain number density and average grain radius. The albedo at each site is taken as the temporal average of the measurements for the measuring period. To investigate the relationship between albedo and snow grain radius, we calculate the vertical mean (VM) grain radius, considering the snow grain size change in a vertical profile, so that a single value of grain radius can be paired with the measured albedo for each site. For this purpose, three models of VM grain size are proposed to investigate whether the statistical relationships between albedo and snow physical parameters are sensitive to the choice of grain radius averaging methods.

[10] The first model is called equal-number-density VM grain radius model (EN model); that is, the total physical mass and the total snow grain number in a unit volume are kept constant in calculating the VM grain radius. For the j th layer ($j = 1$ is the top 3 cm layer), the average equal-number-density composite grain radius or single grain radius is given as

$$\langle r_j^{EN} \rangle = \frac{1}{3 \sqrt{\sum_i \frac{p_{j,i}}{r_{j,i}^3}}} \quad (1a)$$

where $r_{j,i}$ is the measured mean radius of the i th snow particle type (clusters, facets, striates, etc.) within the j th layer (from the top, each 3 cm is sampled and is thus called a layer), and $p_{j,i}$ is the measured relative mass percentage of the i th snow particle type to the whole sample of each category (composite grain or single grain) in the j th layer; $r_{j,i}$ and $p_{j,i}$ were measured and documented for each sample from each snow pit (see Appendix A). The methodology and results were published elsewhere [Morris and Jeffries, 2001]. For the top n layers ($n = 1$ is the top 3 cm snow layer), the equal-number-density VM grain radius for each category (composite or single grains) is given as

$$\bar{r}_n^{EN} = \left(\frac{\sum_{j=1}^n \rho_{j,snow}}{\sum_{j=1}^n \sum_i \frac{p_{j,i} \rho_{j,snow}}{r_{j,i}^3}} \right)^{1/3} \quad (1b)$$

where $\rho_{j,snow}$ is the snow mass density in the j th layer.

[11] The second model is called size-distribution integrated VM grain radius model (DI model). The average distribution-integrated composite grain radius or single grain radius of the j th layer is given as

$$\langle r_j^{DI} \rangle = \frac{\int r f_j(r) dr}{\int f_j(r) dr} = \frac{\sum_i r_{j,i} f_j(r_{j,i})}{\sum_i f_j(r_{j,i})} = \sum_i \left(\frac{p_{j,i}}{r_{j,i}^2} \right) / \sum_i \left(\frac{p_{j,i}}{r_{j,i}^3} \right) \quad (2a)$$

where $f_j(r)$ is the snow particle size distribution function in the j th layer (see Appendix A). This is the statistical mean of radius if the size distribution is given. The size-distribution-integrated VM grain radius for the top n layers for either composite grains or single grains is given as

$$\bar{r}_n^{DI} = \left(\frac{\sum_{j=1}^n \frac{\rho_{j,snow}}{\langle r_j^{DI} \rangle^2}}{\sum_{j=1}^n \frac{\rho_{j,snow}}{\langle r_j^{DI} \rangle^3}} \right) \quad (2b)$$

[12] The third model is called effective VM radius model (EFF model), in which the effective mean radius is proportional to the volume/surface area ratio. For the j th layer, the effective mean radius is (see Appendix A)

$$\langle r_j^{EFF} \rangle = \frac{\int r^3 f_j(r) dr}{\int r^2 f_j(r) dr} = \frac{\sum_i p_{j,i}}{\sum_i \frac{p_{j,i}}{r_{j,i}}} = 1 / \left(\sum_i \frac{p_{j,i}}{r_{j,i}} \right) \quad (3a)$$

The effective VM grain radius for the top n layers for either composite grains or single grains is thus defined as

$$\bar{r}_n^{EFF} = \frac{\sum_j^n \rho_{j,snow}}{\sum_j^n \sum_i^i \frac{\rho_{j,i} \rho_{j,snow}}{r_{j,i}}} \quad (3b)$$

where $\rho_{j,snow}$ is the snow mass density of the j th layer. It is obtained from the mass of each sample and the constant volume (100 cm³) of the cutter by which the snow sample is taken. *Hansen and Travis* [1974] found that disperse media with different particle size distributions but the same effective radius have approximately the same light scattering and absorption characteristics. Other researchers also used the effective optical radius or effective grain size to represent nonspherical ice grains in the discussion of absorption and scattering of electromagnetic radiation by snowpacks. For instance, *Grenfell and Warren* [1999], *Neshyba et al.* [2003], and *Grenfell et al.* [2005] found that nonspherical ice particles (long circular cylinders, solid hexagonal prisms, and hollow hexagonal prisms) can be well represented by a collection of independent spheres for scattering and absorption of radiation based on the effective radius model. From the view point of measurement, *Gay et al.* [2002] proposed the mean convex radius based on skeletization image processing technique as the mean radius of snow grains or clusters of gains. In this work, we will examine the correlation between albedo and each of the statistically derived VM grain radii discussed above.

[13] When the average composite grain radius and single snow grain radius are obtained from equations (1a), (2a), and (3a), the average number density of snow grains in the j th layer for each category can be calculated by

$$n_j^k(\langle r \rangle) = \frac{3\rho_{j,snow}}{4\pi\rho_{ice}\langle r_j^k \rangle^3}, \quad (4a)$$

where ρ_{ice} is the mass density of pure ice, $k = \text{EN, DI or EFF}$ model, and $\langle r_j^k \rangle$ is given in equations (1a), (2a), and (3a). The VM number density of snow grains within the top n layers takes the form as

$$n_n^k(\bar{r}) = \frac{3 \sum_{j=1}^n \rho_{j,snow}}{4\pi n \rho_{ice} (\bar{r}_n^k)^3}, \quad (4b)$$

where \bar{r}_n^k ($k = \text{EN, DI or EFF}$ model) is given by equations (1b), (2b), and (3b).

[14] Regression analyses of the spatial variation of albedo and snow physical parameters, and correlation analyses between albedo and composite grain size, single snow grain size, mass density, and snow grain number density are performed. Correlation coefficients (R) are calculated using Pearson's product-moment correlation statistical method [*Pearson and Hartley*, 1966].

3. Observations of Snow Cover Characteristics

[15] Snow on sea ice generally shows specific characteristics in snow thickness and its spatial distribution, size

distribution, stratigraphy, mass density, shape and size of snow grains, wetness, salinity, and thermal conductivity [*Massom et al.*, 2001]. During the 1999 summer season, snow surface temperature was observed to oscillate about 0°C, causing the melt-refreeze metamorphism to proceed quickly. During the warm phases (~0°C), the liquid water content in the snow resulting from snowmelt takes the form as a coated layer [*Green et al.*, 2002] or collects at points of contact between grains in pendulum or funicular regimes [*Colbeck*, 1979, 1982, 1986], forming clusters from snow single grains. During the subsequent freezing phase (<0°C), the liquid water connecting single grains will be frozen, resulting in consolidated clusters [see *Colbeck*, 1979, Figure 4; *Colbeck*, 1982, Figure 3]. The bonds between single grains are strong because of the resulting continuity between snow grains although individual crystals (single grains) are visible, or partially visible, at this stage. After multiple thaw-refreezing cycles, these clusters will transform into single multicrystalline (melt-freeze) grains of much larger grain radius [*Colbeck*, 1982, Figures 21 and 22; *Colbeck*, 1986, Figure 2]. During the melt-refreeze cycles, clusters of snow grains from a single or a few cycles and multicrystalline melt-freeze grains from multiple cycles may combine to form a mixed cluster [*Colbeck*, 1986, Figure 3]. Because of frequent melt-refreezing cycles, summer snow cover on Antarctic sea ice is characterized by ubiquitous icy melt-refreeze clusters with grain size of 1 cm order, as well as ice lenses, ice layers, and percolation columns [*Haas*, 2001; *Morris and Jeffries*, 2001].

[16] Composite grains as new entities form from single grains by melt-refreezing and recrystallization processes etc. These composite grains include clustered single crystals, melt-freeze polycrystalline particles [*Colbeck et al.*, 1990], and the mixture of both, makes the summer snowpack on sea ice a unique snow cover with coarse (1.0–2.0 mm) or even extremely coarse (>5 mm) grain size distribution. *Morris and Jeffries* [2001] found that snow composite grains constitute most (~66%) of the snowpack on Antarctic sea ice in summer while individual (separate) single grains account for only a small portion. The centimeter-scale composite grains in snow were also observed in winter, after a surface-melt-freezing cycle due to infrequent warm storms and subsequent refreezing [*Massom et al.*, 1998].

4. Spatial Variations of Albedo and Snow Physical Parameters

[17] Twenty five data sets of albedo were collected (Figure 1), of which 19 data sets (open circles in Figure 1) from the central pack ice are used for analyses. The other 6 ice stations (solid circles in Figure 1) at the ice edges generally had very low ice concentrations, and are excluded from the analyses because the field of view of the pyranometers contained open water. All ice stations have snow depth greater than 9 cm.

4.1. Latitudinal Variation of Snow Grain Size and Snow Grain Number Density

[18] The latitudinal variation of mean snow grain radius (DI Model) of the top 3 cm of the snowpack, calculated using equation (2a), is shown in Figure 2. Correlation coefficients and significances (s) are shown in Table 1.

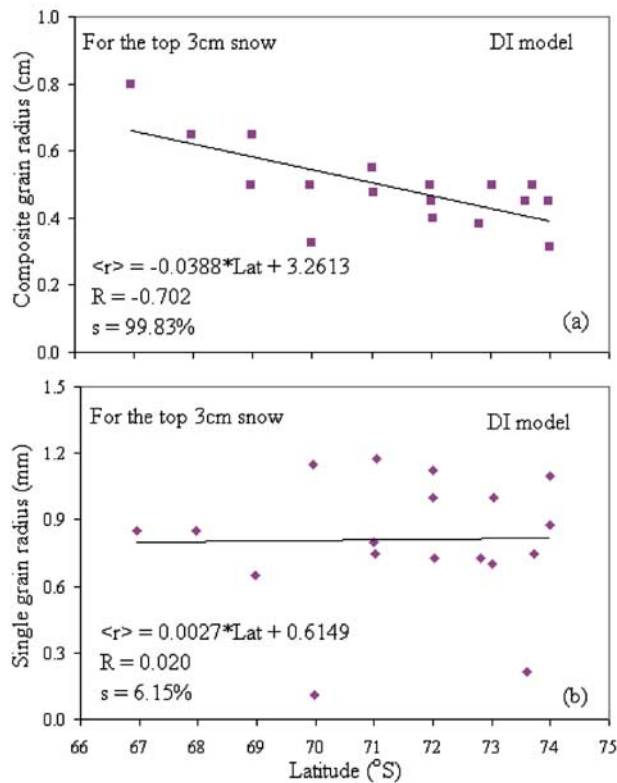


Figure 2. Latitudinal variation of (a) composite grain VM radius and (b) single grain VM radius of the top 3 cm snow. With an increase in latitude south, snow composite VM grain radius shows a negative correlation, while no correlation is found between single VM grain radius and latitude.

Here significance is defined as $s = (1 - p) \times 100\%$, where p is the level of probability for the rejection of the null hypothesis with correlation coefficient $R = 0$. All three models for the calculation of the mean grain radius show similar results. The mean composite grain radius of the top 3 cm snow cover calculated with the three size models decreases with increasing latitude. The effect of depth on the correlation coefficient and level of significance is also shown in Table 1. Correlation between composite grain radius and latitude is observed to be significant (i.e., the significance value, s , greater than the threshold 95%) only for the top 3 cm snow. We also observed that for any average radius model, the correlation coefficients of the composite grain radius with latitude decrease from the first layer (top 0–3 cm) down to the third layer (6–9 cm from top). The mean single grain radius calculated from the three average models are not observed to correlate significantly with latitude for any depth layer.

[19] From the above spatial analysis on snow grain radius, we can see that the mean composite radius of only the top layer (0–3 cm) is correlated with latitude for the snowpack in the Ross Sea, the lower layers are not. This may indicate that the composite grain radius of the top 3 cm snow layer is more sensitive to meteorological processes, especially the temperature-dependent melt-refreeze metamorphism (see temperature change with latitude in section 4.2), as compared to the lower layers in the snow cover.

[20] Snow composite grain number density and single grain number density in each layer were calculated using equation (4a). No correlation between latitude and composite and/or single grain number densities in any depth layer is found to be significant. The lack of correlation between snow mass density and latitude (see section 4.2) explains this observation because number density is a derivative of snow grain size and mass density.

4.2. Latitudinal Variation of Snow Surface Albedo, Surface Temperature, and Mass Density

[21] The relationships between albedo, surface temperature, and mass density of the top 3 cm with latitude are shown in Figure 3. Albedo is positively correlated with latitude, while surface temperature and mass density of the top 3 cm snow are negatively correlated; hence snow surface albedo increases with latitude, while surface temperature and snow mass density of the top 3 cm decrease.

[22] The spatial variation of temperature with latitude is understandable considering the effect of the colder continent as compared with the warmer ocean, although the overall daily receipt of solar radiation by the snowpack from north to south does not vary much from 66°S to 75°S in January and February as a consequence of latitude difference [Liou, 1980]. The likely cause of the variation in solar radiation over the range of latitudes is the change in the average total cloud cover from 85% to 65% and 89% to 74% in this region in January and February respectively (i.e., fewer clouds at higher latitude) [Warren et al., 1988].

[23] In contrast to the surface (0–3 cm) snow density, the correlation between the mass density of snow below the top 3 cm and latitude is not significant, similar to composite grain size. This may indicate that the mass density and composite grain size at the very top layer of snowpack (≤ 3 cm) is more sensitive to the surface meteorological processes, but the layers below are not. This is understandable since the very top snow layer is the first to receive impacts from surface meteorological processes such as air temperature change which can be spatially variable and can result in temperature-related metamorphism. The latitudinal variation of the mass density of the top 3 cm is significant but the correlation coefficient ($R = 0.49$) is not as high in magnitude as composite grain size ($R = -0.66$). This may indicate some role is played by large-scale meteorological

Table 1. Correlation Coefficients and Significance Between Composite Grain VM Radius and Latitude (in Degree) Within Different Depth Layer for the Three Average Radius Models

Snow Depth	EN Model $\langle r^{EN} \rangle$	DI Model $\langle r^{DI} \rangle$	EFF Model $\langle r^{EFF} \rangle$
0–3 cm	$R = -0.701, s > 99\%$	$R = -0.702, s > 99\%$	$R = -0.698, s > 99\%$
3–6 cm	$R = -0.401, 80\% < s < 90\%$	$R = -0.404, 80\% < s < 90\%$	$R = -0.397, 80\% < s < 90\%$
6–9 cm	$R = -0.373, 80\% < s < 90\%$	$R = -0.375, 80\% < s < 90\%$	$R = -0.372, 80\% < s < 90\%$

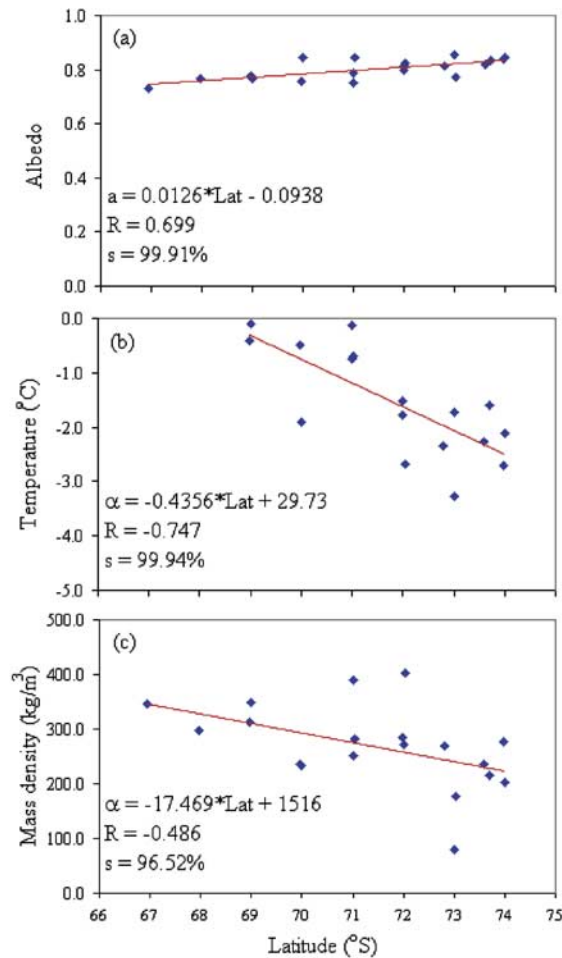


Figure 3. Spatial variation of (a) albedo, (b) snow surface temperature, and (c) snow mass density of the top 3 cm, with respect to the latitude in degree on the pack ice in the Ross Sea.

processes such as wind stress etc., which could result in snow settling processes and densification, but not much in grain size. The measurement may be within the scale of these meteorological processes, resulting in the reduction of correlation with latitude for mass density, but not for composite grain size.

5. Relationship of Albedo With Snow Physical Parameters

[24] To accurately parameterize snow surface albedo in climate and snowmelt-runoff modeling studies, the relationships of albedo with various snow physical parameters are imperative. In the following discussion, albedo as a function of grain size, grain number density, snow mass density, and stratification is studied, providing some insights in albedo parameterization.

5.1. Albedo as a Function of Grain Size

[25] The relationships of albedo with composite grain VM radius and composite grain VM number density are analyzed for multiple layers so that effects of the snow stratification on albedo can be unveiled. The VM grain

radius (for both composite and single grains) within multiple layers is calculated using equations (1b), (2b), and (3b). The mean number density of each layer and the VM number density in multiple layers are evaluated using equations (4a) and (4b), respectively. Snow mass density is the measured data and the mean grain radius in each layer is calculated using equations (1a), (2a), and (3a), as have been done in section 4.

[26] Relationships between albedo and VM composite grain radius calculated for different depths of snow (up to 9 cm) are shown in Figures 4a–4c. Only results from EFF model are shown as the other two models produce similar results. Albedo is observed to vary significantly with the VM composite grain radius in the top 3-cm snow: it decreases with increase of composite grain size. Results from all three models show high correlation coefficient $R = -0.79 \pm 0.009$. For snow layer of the top 6 cm, all models show a correlation coefficient of $R = -0.72 \pm 0.003$ with $s > 99\%$ and for snow layer of the top 9 cm, $R = -0.66 \pm 0.01$ with $s > 99\%$. Significant correlation between albedo and composite grain radius remains up to the top 9 cm snow. Further increase of snow depth has little effect on albedo, which indicates that the snowpack approaches its semi-infinite depth for albedo as the snow depth reaches 9–12 cm. These results agree well with a multilayer radiative transfer modeling that the top 10 cm of a similar snowpack (snow density $\sim 300 \text{ kg/m}^3$; $\langle r \rangle \sim 1 \text{ mm}$) contribute to albedo by greater than 97% [Zhou et al., 2003a].

[27] Relationships between albedo and VM single grain radius calculated for different depths of snow (up to 9 cm) are shown in Figures 4d–4f. Only results from the EFF model are shown as the other two models produce similar results. For example, the correlation coefficient between albedo and single grain VM radius for the top 3 cm snow derived from the three models is $R = -0.16 \pm 0.06$ with $s < 50\%$. We also observed that the correlation coefficient and significance level both increase as snow depth increase from 3 cm to 9 cm. However, for single grains, albedo is not observed to vary significantly with single grain VM radius for any of the snow depths we analyzed. This indicates that the size of clusters of snow grains, rather than the size of the individual snow grains, is the dominant parameter controlling albedo of the snow cover on sea ice in the summer time in the Ross Sea.

5.2. Albedo as a Function of Number Density

[28] From scattering theory [Bohren and Huffman, 1983], the number density is also a quantity directly controlling scattering coefficient. Relationships between albedo and composite grain VM number density (EFF model) for various depths of snow (up to 9 cm) are shown in Figures 5a–5c. For the top 3 cm of snow, albedo is observed to vary significantly with VM composite grain number density calculated (all models). However, the correlation coefficient and significance at each depth are not as high as those for the relationship between albedo and composite grain radius (Figure 4). Results from all the three models show that for each depth of snow that is less than 6 cm, albedo is significantly correlated with composite grain number density: the larger the number density is, the higher the albedo is. For a snow depth of 9 cm, the relationship between albedo and composite grain number

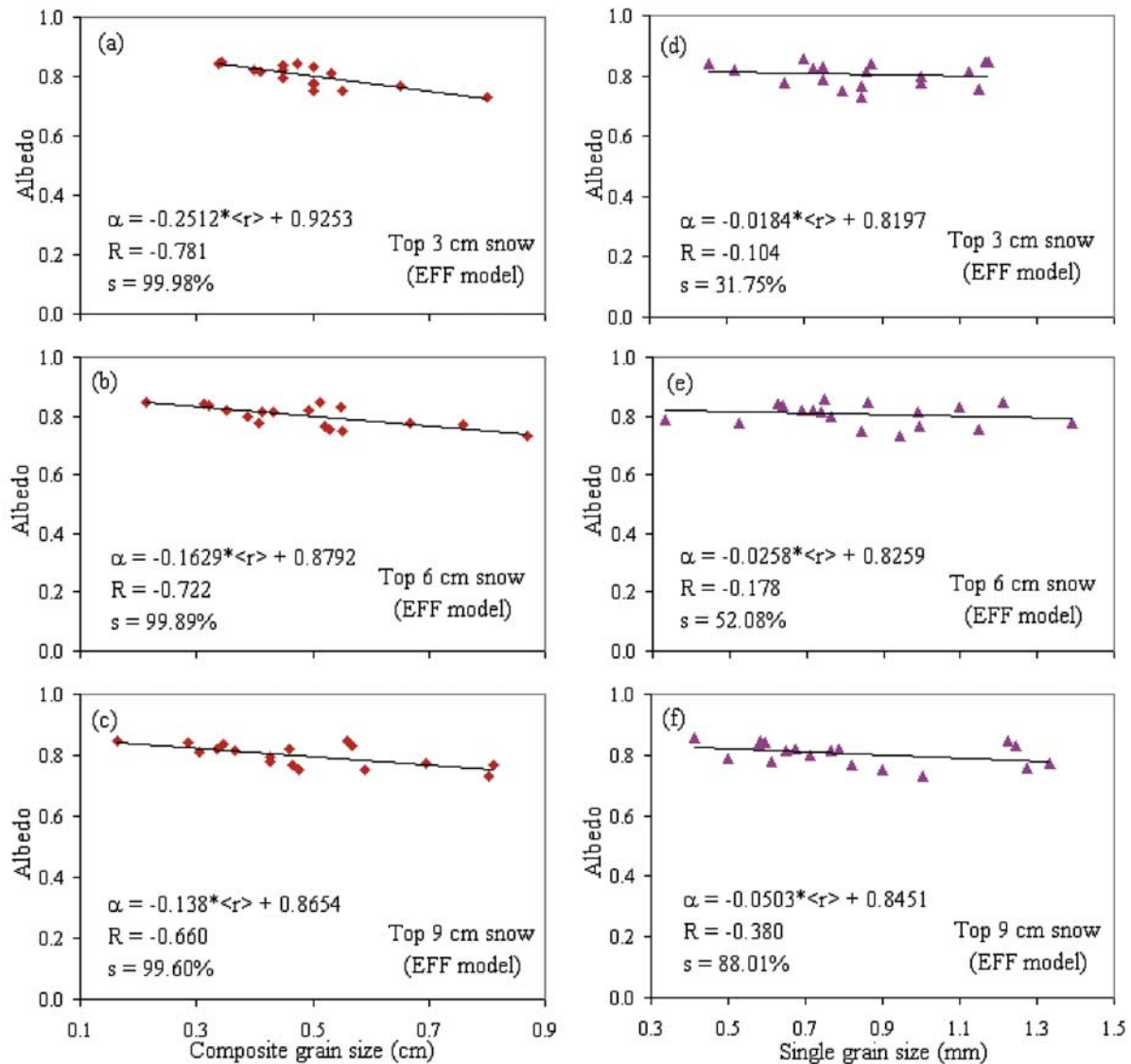


Figure 4. Variation of albedo (α) with snow composite grain VM radius and snow single grain VM radius ($\langle r \rangle$) for various depths of snow cover. Albedo versus snow composite grain VM radius for snow depth (a) $d = 3$ cm, (b) $d = 6$ cm, and (c) $d = 9$ cm. Albedo versus snow single grain radius for snow depth (d) $d = 3$ cm, (e) $d = 6$ cm, and (f) $d = 9$ cm. Results shown here are from EFF model. The EN and DI models produced similar results.

density is significant for the EFF model; significance values from the other two models are a little bit lower than the threshold 95%. Results from all three models show that a significant correlation between albedo and composite grain VM number density remains up to the top 9 cm snow, which is similar to the grain size case. Relationships between albedo and single grain VM number density (EFF model) for various depths of snow (up to 9 cm) are shown in Figures 5d–5f. Analyses for single grain VM number density show that albedo does not vary with single grain VM number density for any snow depth. Combined with the discussion on the relationship between albedo and grain radius (see section 5.1), it is reasonable to take 9–12 cm as the depth of active light scattering layer since the sampling resolution in this study is 3 cm. The

significant correlation between albedo and composite grain number density may indicate the importance of the number density of scatters to the surface albedo within the scattering layer. Correlation analyses of albedo with average snow mass density for snow depth from 3 cm up to 15 cm show that no significant correlation exists between albedo and mass density at any depth. These results are in line with the conclusions made by *Bohren and Beschta* [1979] and *Zhou et al.* [2003a].

5.3. Albedo as a Composite Function of Grain Size and Number Density

[29] From the above analyses it has been seen that albedo is strongly correlated with composite grain VM radius and composite VM number density for a snow

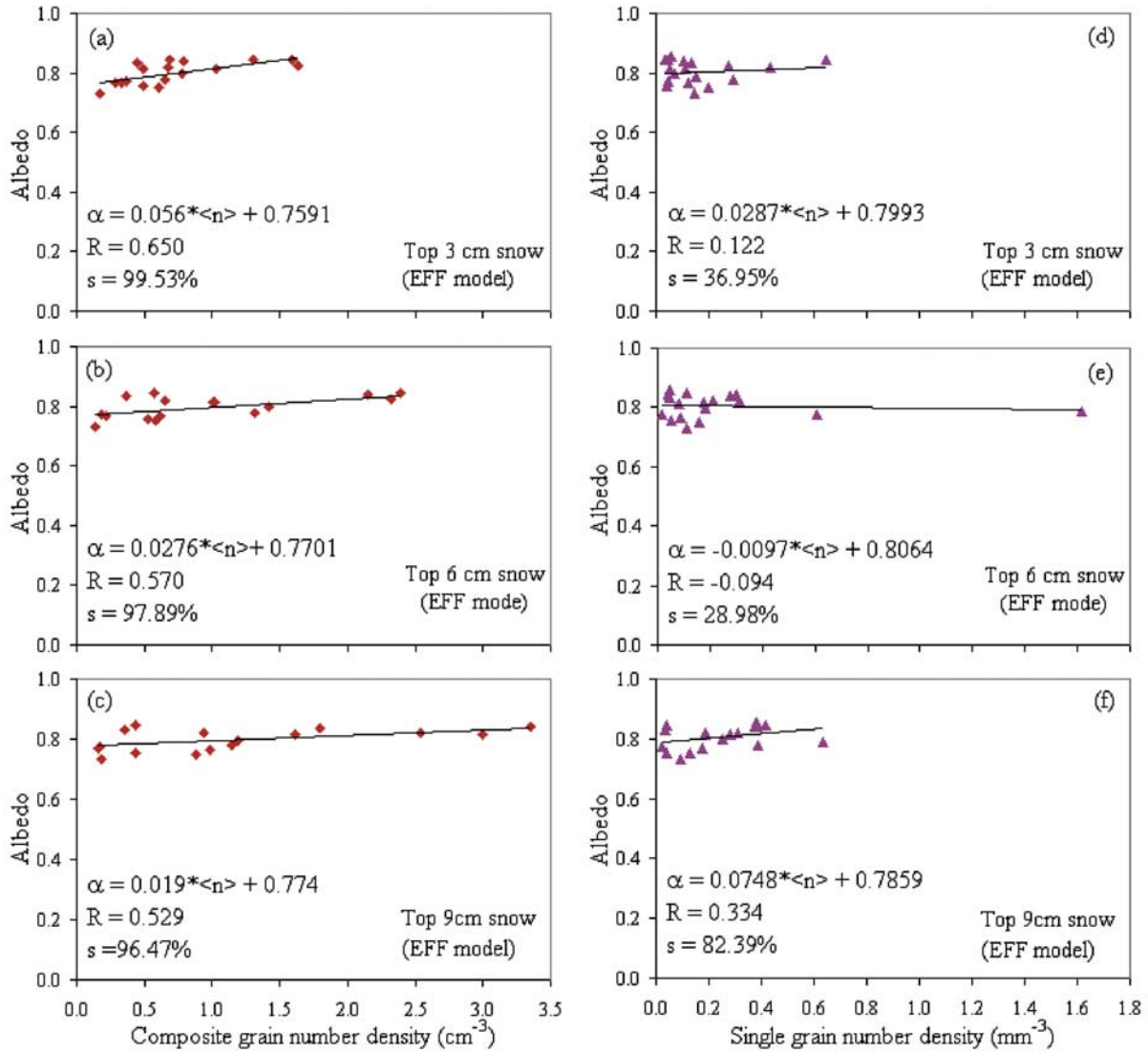


Figure 5. Relationship between albedo (α) and snow composite grain VM number density and single grain number density ($\langle n \rangle$) for various depths of snow. Albedo versus snow composite grain number density for snow depth (a) $d = 3$ cm, (b) $d = 6$ cm, and (c) $d = 9$ cm. Albedo versus snow single grain number density for snow depth (d) $d = 3$ cm, (e) 6 cm, and (f) 9 cm, respectively. Results shown here are from EFF model. The EN and DI models produced similar results.

depth up to 9–12 cm. To assess the effect of both composite grain size and number density at different layers on albedo, and to separate statistically the contributions to albedo by composite grain VM radius and VM number density, a multivariate regression analysis is performed.

[30] The analysis results show that the three structurally based snow grain average models result in essentially the same results (e.g., see Table 1). The results are not sensitive to the integration method for VM grain radius calculation. Therefore, in the following discussion for a multivariate analysis of albedo with composite grain radius and number density, we select the VM results calculated by the EFF model. We have seen from previous sections that albedo is not correlated significantly with single grain VM radius and single grain VM number density. Thus we only discuss the composite grain case.

[31] A multiple regression equation linking albedo (α) with composite grain size ($\langle r \rangle$) and number density ($\langle n \rangle$) is given as follows following Williams [1992]

$$\alpha = a + b_{\langle r \rangle \alpha, \langle n \rangle} \langle r \rangle + b_{\langle n \rangle \alpha, \langle r \rangle} \langle n \rangle \quad (5)$$

where a , $b_{\langle r \rangle \alpha, \langle n \rangle}$, and $b_{\langle n \rangle \alpha, \langle r \rangle}$ are coefficients. Here grain radius and number density are treated theoretically as independent variables because snowpacks with the same grain radius can have different degrees of densification, and thus different mass densities and number densities. The statistical significance of the multivariate analyses is tested with an F test [Pearson and Hartley, 1966]. Values of coefficients a , $b_{\langle r \rangle \alpha, \langle n \rangle}$, $b_{\langle n \rangle \alpha, \langle r \rangle}$, correlation coefficients $R_{\alpha, \langle r \rangle \langle n \rangle}$ of albedo (α) as a function of composite grain VM radius ($\langle r \rangle$) and VM number density ($\langle n \rangle$), and

Table 2. Results of Multivariate Regression of Albedo With Composite Grain VM Grain Size and Number Density Calculated Using the EFF Model^a

	Snow Depth		
	3 cm	6 cm	9 cm
a	0.9155	0.8794	0.8593
$b_{(r)\alpha,(n)}$	-0.2372	-0.1602	-0.1288
$b_{(n)\alpha,(r)}$	1.7924×10^{-3}	1.7744×10^{-3}	1.0869×10^{-3}
$R_{\alpha(r)(n)}$	0.788	0.682	0.608
Significance	>99.5%	>97.5%	>95.0%
Total albedo predicted	61.0%	52.1%	37.0%
From composite grain size	58.3%	51.0%	35.4%
From composite grain number density	2.7%	1.1%	1.6%

^aPercentages of the predicted albedo from each of the two components are also included.

significance (s) of the correlation for the top 3 cm, 6 cm, and 9 cm snow are shown in Table 2. Significance values (95% level) in Table 2 show that albedo as a function of composite grain size and number density (equation (5)) holds for snow depth up to 9 cm. Beyond 9 cm, it is not significant. For the top 3 cm of the snow cover, the EFF model results (other model results are similar) indicate that approximately 58.3% of the predicted albedo (total 61.0%) is accounted for by composite grain size and approximately 2.7% is due to the composite grain number density. For the top 6 cm snow, approximately 51.0% of the predicted of albedo (total 52.1%) is accounted for by composite grain size and about 1.1% is due the number density. For the top 9 cm snow, approximately 35.4% of the predicted of albedo (totally 37.0%) is accounted by composite grain size and about 1.6% is due to the number density.

[32] Correlation analysis between snow composite radius and grain number density for the top 3 cm snow layer results in a correlation coefficient of -0.815 , which indicates that for the natural snowpack as observed in the Ross Sea, the independence of snow grain size and snow grain number density is very limited. This may explain why the predicted albedo is dominated by composite grain size over the composite grain number density.

5.4. Albedo as a Composite Function of Grain Size at Different Layers

[33] Now we investigate the effect of snow stratification on snow albedo by focusing on the composite grain size at different layers. Correlation analyses of albedo with composite grain radius at each individual layer (0–3 cm, 3–6 cm and 6–9 cm layers) show that albedo is correlated with composite grain radius in each individual layer. For the 0–3 cm layer, $R = -0.781$ with $s > 99.9\%$; for the 3–6 cm layer, $R = -0.632$ with $s > 95\%$; and for the 6–9 cm layer, $R = -0.491$ with $s > 95\%$. Regression analyses of the data sets show that multivariate regression equation of albedo with composite grain size in different layers is given as

$$\alpha = 0.9197 - 0.2187 \langle r_{0-3}^{EFF} \rangle - 2.707 \times 10^{-2} \langle r_{3-6}^{EFF} \rangle + 5.985 \times 10^{-3} \langle r_{6-9}^{EFF} \rangle \quad (6)$$

with the multiple correlation coefficient $R = -0.786$ with $s > 99\%$. This indicates that the multivariate regression relation (6) is significant for fitting the field data sets. From the ratios of coefficients $0.2187:2.707 \times 10^{-2}:5.985 \times 10^{-3} \approx 36.5:4.5:1$, we can see that the contribution of the top layer (0–3 cm) is 36.5 times that of the third layer (6–9 cm) (86.9% of the total) and the contribution of the second layer (3–6 cm) is 4.5 times that of the third layer (10.7%) if the average composite grain radius of all the three layers are the same. These results translate into another set of statistics: the top 3 cm snow contributes to about 86.9% of the snow albedo, and the top 6 cm snow layer 97.7% when the top 9 cm is assumed to contribute 100% to albedo.

[34] All these results show that for the albedo measured on a snow surface of sea ice, the contribution from the snow grain size dominates over that of snow number density, and the contribution from the top 6 cm dominates over the snow layers below. A 9–12 cm depth of snow can be considered semi-infinite.

6. Discussion and Conclusions

[35] On the basis of the snow albedo and snow pit data collected on the snow cover of sea ice from a summer cruise (NBP99-01) in the Ross Sea (sector 135°W to 166°W) in 1999, correlation analyses show that albedo increases southward in the central pack ice as snow composite grain radius decreases. *Brandt et al.* [2005] used albedo measurements from 3 Antarctic cruises [*Allison et al.*, 1993; *Brandt et al.*, 2005], in conjunction with snow and sea ice characterizations from the Antarctic Sea Ice Processes and Climate (ASPeCt) database [*Worby and Allison*, 1999; *Worby and Dirita*, 1999], to explore the relationship between albedo and latitude in the Ross Sea (sector 160°E to 130°W). They synthesized the albedo data from these cruises and assign a specific albedo value (average value) to a specific ice type under specific sky conditions [*Brandt et al.*, 2005, Table 1]. They found that the area-averaged albedo increases from the northern ice edge to the central pack ice and then decreases to the southern ice edge because of regional variation of ice concentration, but the ice-only albedo is nearly independent of latitude. This differs somewhat from our observation that snow covered ice-only albedo increases southward with latitude through the central pack ice, although we also observed the albedo drops at the southern ice edge. This difference may be due to the fact that *Brandt et al.* [2005] used averaged albedo values thus eliminating the site-to-site impact of grain size on the in situ albedo measurements. Snow surface temperature shown in this study was collected during the day. Snow surface temperature decreases with latitude from north to south on the pack ice. Spatial temperature differences can cause different metamorphism (including melting-refreezing) rates: higher temperature will lead to coarser snow grains. From Figure 3, we can see that the temperature fluctuates between 0 to -4°C . As melting generally occurs during the day time while refreezing occurs during the nighttime, the sites on the sea ice that have higher temperature during the day will have a higher probability of occurrence of melting-refreezing cycles. As a consequence, the more composite grains and larger grains will be formed. Latitudinal variation of snow composite grain size from

Table 3. Relationships of Albedo With Latitude, Composite Grain Size and Density, and Stratification for a Semi-Infinite Snowpack (≥ 9 cm) Using the EFF Model

Parameter(s)	Albedo: α	Verified Valid Range
Latitude, °S: Lat	$\alpha = 0.0126 * Lat - 0.0938$	Lat \in (66, 75) °S
Grain radius, cm: $\langle r \rangle$	$\alpha = -0.1380 \langle r \rangle + 0.8654$	$\langle r \rangle \in$ (0.1, 0.9) cm
Number density, cm ⁻³ : $\langle n \rangle$	$\alpha = 0.0190 \langle n \rangle + 0.7740$	$\langle n \rangle \in$ (0, 3.5) cm ⁻³
$\langle r \rangle$ and $\langle n \rangle$	$\alpha = 0.8593 - 0.1288 \langle r \rangle + 1.0869 \times 10^{-3} \langle n \rangle$	
$\langle r \rangle$ in 3 layers	$\alpha = 0.9197 - 0.2187 \langle r_{0-3} \rangle - 2.707 \times 10^{-2} \langle r_{3-6} \rangle + 5.985 \times 10^{-3} \langle r_{6-9} \rangle$	

north to south represents the spatial variation of melting, wetting, and refreezing in the snowpack in the Ross Sea. Snow mass density is a strong function of snow type ranging from 108 kgm⁻³ for new snow to greater than 760 kgm⁻³ for icy layers [Sturm *et al.*, 1998] and a function of metamorphosis process as well [Haas, 2001; Morris and Jeffries, 2001]. Snow mass density of the top snow layers are observed to decrease with increasing latitude from north to south on the pack ice. This indicates that the densification is less at higher latitude on the pack ice. Snow mass density is also observed to correlate with composite grain radius: snowpacks with higher mass densities have larger composite grain radii. The composite grain number density is not strongly correlated with latitude. It is observed that snow composite grain radius of the top 3 cm snow decreases with latitude from north to south. The composite grain number density is not found to correlate significantly with latitude. The correlation analyses between albedo and snow grain size show that albedo increases with decreasing composite grain radius and increasing number density within the upper most 9 cm of the snow cover. No such relation is observed between albedo and single grain radius and single grain number density at any depth of snow. The strong correlation of albedo with composite grain radius and number density indicates that the strong grain bonds in the formation of composite grains may play an important role in determining optical properties of summer snow such as albedo. The albedo-grain size relationship was studied by other researchers [e.g., Wiscombe and Warren, 1980; Grenfell *et al.*, 1994; Perovich *et al.*, 2002; Aoki *et al.*, 2003], their general conclusion was that the albedo decreases with snow grain size. The unique finding of our study is that the general relationship between albedo and snow grain size is valid only for snow composite grains not for single grains as observed on the austral snowpack in Ross Sea, indicating the impact of the much larger composite grains.

[36] Multivariate correlation analysis of albedo with composite grain radius and number density shows that albedo does have a relationship with both composite grain radius and number density. However, evaluation of contributions of predictor variables indicates that for a prediction of albedo, grain radius is a dominant contributor. For a 9 cm thick homogeneous snow cover, within the variation of albedo due to change in grain radius, the top layer (0–3 cm) contributes approximately 86.9% to the total albedo, while the 3–6 cm layer accounts for about 10.7%, and the 6–9 cm layer adds 2.4%. Since the sampling resolution in this study is 3 cm, the top 9–12 cm snow is thus the most important for the optical properties of a snowpack of greater depth.

[37] On the basis of the data analyses, for a snow cover over sea ice, position, snow depth, composite grain size,

composite grain number density, and vertical distribution of grain size appear to be important factors to be considered in albedo parameterization schemes. Some parameterization schemes with verified valid variable ranges are shown in Table 3.

[38] The effects of clouds were not considered in this study. It has been found by others [Perovich *et al.*, 2002] that albedo is related to sampling time when it spans long periods. In this study, when albedo was plotted against date no consistent relationship was found, perhaps because of the relatively short period of time (January and February). The albedo parameterizations employed here should only be used to examine the effects of composite grain size on albedo. They may not properly represent all-wave albedo versus latitude in the Ross Sea region under a range of atmospheric conditions (i.e., cloud cover). In addition, these parameterizations are for snow covered sea ice; leads within the ice pack, which may represent a large area, need to be accounted for using other albedo values.

[39] In summary, (1) as albedo increases, snow surface temperature and mass density of the top 3 cm snow decreases with increasing latitude on the central pack ice in the Ross Sea. (2) Composite grain radius decreases only within the top 3 cm of snow with increasing latitude, and latitude dependence is not observed for single grain radius and single grain number density at any depth. (3) The size of the clusters of snow grains, rather than the size of the individual single snow grains, is the dominant parameter controlling albedo. (4) Contribution to the prediction of albedo by snow grain size and snow grain number density is dominated by composite grain radius. (5) In the determination of snow albedo, grain size dominates over the number density; the upper layers over the lower layers. (6) A comparison of statistical relation between albedo and grain size/number density using three different snow grain size averaging models indicates that statistical significance is not sensitive to the model selection.

Appendix A

A1. Equal-Number-Density VM Radius Model (EN Model)

[40] For the equal-number-density VM grain radius model (EN model), we assume that the total physical mass and the total snow grain number in a unit volume are conserved before and after averaging. For the j th layer ($j = 1$ is the top 3 cm layer), assume the mass is w_j and the total number of snow grains is N_j in a unit volume. Before averaging, since the mean radius $r_{j,i}$ and the relative mass

percentage $p_{j,i}$ of the i th snow particle type (clusters, facets, striates, etc.) within the j th layer are measured, the total number of snow grains in a unit volume (or number density) is calculated as

$$N_j = \sum_i \frac{p_{j,i} w_j}{\frac{4\pi}{3} r_{j,i}^3 \rho_{ice}} \quad (\text{A1})$$

where ρ_{ice} is the mass density of pure ice. After averaging, the average composite grain radius or single grain radius is $\langle r_j^{EN} \rangle$ and thus the total number of grains in a unit volume is

$$N_j = \frac{w_j}{\frac{4\pi}{3} \langle r_j^{EN} \rangle^3 \rho_{ice}} \quad (\text{A2})$$

Since the number density is assumed equal before and after the averaging procedure, we have the average equal-number-density composite grain radius or single grain radius in the j th layer as given in equation (1a).

[41] For the case of n vertical layers of a snowpack, in each layer we consider a unit volume. Thus we have a column of n unit volumes. The mass in each unit volume is the snow density corresponding to the layer. The total mass (w) and number of snow grains (N) in the column derived from the measurement of mean snow grain radius, relative mass percentage, and snow density in each layer are, respectively

$$w = \sum_{j=1}^n \rho_{j,snow} \quad (\text{A3})$$

$$N = \sum_{j=1}^n \sum_i \frac{p_{j,i} \rho_{j,snow}}{\left(\frac{4\pi}{3} r_{j,i}^3\right) \rho_{ice}} \quad (\text{A4})$$

where $\rho_{j,snow}$ is the mass density of snow in the j th layer. After averaging along the vertical profile, if the vertical mean radius is denoted as \bar{r}_n^{EN} , the total number of grains is

$$N = \frac{w}{\frac{4\pi}{3} (\bar{r}_n^{EN})^3 \rho_{ice}} = \frac{\sum_{j=1}^n \rho_{j,snow}}{\frac{4\pi}{3} (\bar{r}_n^{EN})^3 \rho_{ice}} \quad (\text{A5})$$

Since the snow grain number density is assumed to be equal during the averaging procedure, the total number of snow grains in the column before and after averaging is equal. We thus have the equal-number-density VM grain radius as given in equation (1b).

A2. Size-Distribution Integrated VM Radius Model (DI Model)

[42] Assume the snow particle size distribution function in the j th layer is $f_j(r)$, where r is the radius of snow particles. By definition, the statistical mean of snow grain radius is

$$\langle r_j^{DI} \rangle = \frac{\int r f_j(r) dr}{\int f_j(r) dr} \quad (\text{A6})$$

In the field, the mean grain radius of each types of snow particles (clusters, facets, striates, etc.) were measured, thus $f_j(r)$ is approximated as

$$f_j(r) \approx f_j(r_{j,i}) = \frac{p_{j,i}}{\left(\frac{4\pi}{3} r_{j,i}^3\right) \rho_{ice}} \quad (\text{A7})$$

where ρ_{ice} is the mass density of ice. The right hand side is the number density of snow grains at radius of $r_{j,i}$. Thus we have equation (2a).

[43] For the case of n layers for either composite grains or single grains, the size-distribution function $f_j(r)$ is now the vertical radius profile with the mean radius being $\langle r_j^{DI} \rangle$ and the number density of snow grains being $\frac{\rho_{j,snow}}{\frac{4\pi}{3} \langle r_j^{DI} \rangle^3 \rho_{ice}}$ within the j th layer. Similar to obtaining equation (1b) above, we have the distribution-integrated VM grain radius as given in equation (2b).

A3. Effective VM Radius Model (EFF Model)

[44] For the effective VM radius model (EFF model), the effective mean radius is proportional to the ratio of mean volume ($\sim r^3$) to the mean surface area ($\sim r^2$) of all particles. For the j th layer, the effective mean radius is

$$\langle r_j^{EFF} \rangle = \frac{\int r^3 f_j(r) dr}{\int r^2 f_j(r) dr} \quad (\text{A8})$$

Insert equation (A7) in equation (A8) and considering $\sum p_{j,i} = 1$, we have equation (3a). For the case of n layers for either composite grains or single grains, the size-distribution function $f_j(r)$ is now the vertical radius profile with the mean radius being $\langle r_j^{EFF} \rangle$ and the number density of snow grains being $\frac{\rho_{j,snow}}{\frac{4\pi}{3} \langle r_j^{EFF} \rangle^3 \rho_{ice}}$ within the j th layer. Similar to obtaining equation (2b) above, we have the effective VM grain radius for the top n layers for either composite grains or single grains as given in equation (3b).

[45] **Acknowledgments.** We are very grateful for the logistical support provided by the National Science Foundation and the Antarctic Support Associates personnel on board the R/V *Nathaniel B. Palmer*. This work was supported by NASA under grant NAG5-6338, the National Science Foundation under grant OPP9614844, and Montana Tech Seed Grant. We are very grateful to the three anonymous reviewers for their helpful and constructive comments and suggestions. Thanks also go to Hajo Eicken (University of Alaska Fairbanks, USA) and Teruo Aoki (Meteorological Research Institute, Japan), who once reviewed an earlier version of the manuscript and made many useful comments.

References

- Allison, I., R. E. Brandt, and S. G. Warren (1993), East Antarctic sea ice: Albedo, thickness distribution, and snow cover, *J. Geophys. Res.*, *98*(C7), 12,417–12,429.
- Aoki, T., A. Hachikubo, and M. Hori (2003), Effects of snow physical parameters on shortwave broadband albedos, *J. Geophys. Res.*, *108*(D19), 4616, doi:10.1029/2003JD003506.
- Bohren, C. F., and R. L. Beshta (1979), Snowpack albedo and snow density, *Cold Reg. Sci. Technol.*, *1*, 47–50.
- Bohren, C. F., and D. R. Huffman (1983), *Absorption and Scattering of Light by Small Particles*, 530 pp., John Wiley, New York.
- Bonan, G. B., K. W. Oleson, M. Vertenstein, S. Levis, X. Zeng, Y. Dai, R. E. Dickinson, and Z.-L. Yang (2002), The land surface climatology of the Community Land Model coupled to the NCAR Community Climate Model, *J. Clim.*, *15*(22), 3123–3149.
- Brandt, R. E., S. G. Warren, A. P. Worby, and T. C. Grenfell (2005), Surface albedo of the Antarctic sea ice zone, *J. Clim.*, *18*(17), 3606–3622.

- Colbeck, S. C. (1979), Grain clusters in wet snow, *J. Colloid Interface Sci.*, **72**, 371–384.
- Colbeck, S. C. (1982), An overview of seasonal snow metamorphism, *Rev. Geophys.*, **20**, 45–61.
- Colbeck, S. C. (1986), Classification of seasonal snow cover crystals, *Water Resour. Res.*, **22**(9), 759–768.
- Colbeck, S., E. Akitaya, R. Armstrong, H. Gubler, J. Lafeuille, K. Lied, D. McClung, and E. Morris (1990), *The International Classification for Seasonal Snow on the Ground*, 23 pp., Int. Comm. on Snow and Ice of the Int. Assoc. of Sci. Hydrol., Gentbrugge, Belgium.
- Curry, J. A., J. L. Schramm, D. K. Perovich, and J. O. Pinto (2001), Applications of SHEBA/FIRE data to evaluation of snow/ice albedo parameterizations, *J. Geophys. Res.*, **106**(D14), 15,345–15,355.
- Dai, Y., et al. (2003), The Common Land Model, *Bull. Am. Meteorol. Soc.*, **84**(8), 1013–1023.
- Desborough, C. E., and A. J. Pitman (1998), The BASE land surface model, *Glob. Planet. Change*, **19**(1–4), 3–18.
- Dimhir, I., and F. D. Eaton (1975), Some characteristics of the albedo of snow, *J. Appl. Meteorol.*, **14**, 375–379.
- Gay, M., M. Fily, C. Genthon, M. Frezzotti, H. Oerter, and J. G. Winther (2002), Snow grain-size measurements in Antarctica, *J. Glaciol.*, **48**(163), 527–535.
- Green, R. O., J. Dozier, D. Roberts, and T. Painter (2002), Spectral snow-reflectance models for grain-size and liquid-water fraction in melting snow for the solar-reflected spectrum, *Ann. Glaciol.*, **34**, 71–73.
- Grenfell, T. C., and S. G. Warren (1999), Representation of a non-spherical ice particle by a collection of independent spheres for scattering and absorption of radiation, *J. Geophys. Res.*, **104**(D24), 31,697–31,709.
- Grenfell, T. C., S. G. Warren, and P. C. Mullen (1994), Reflection of solar radiation by the Antarctic snow surface at ultraviolet, visible, and near-infrared wavelengths, *J. Geophys. Res.*, **99**(D9), 18,669–18,684.
- Grenfell, T. C., S. P. Neshyba, and S. G. Warren (2005), Representation of a non-spherical ice particle by a collection of independent spheres for scattering and absorption of radiation: 3. Hollow columns and plates, *J. Geophys. Res.*, **110**, D17203, doi:10.1029/2005JD005811.
- Haas, C. (2001), The seasonal cycle of ERS scatterometer signatures over perennial Antarctic sea ice and associated surface ice properties and processes, *Ann. Glaciol.*, **33**, 69–73.
- Hansen, J. E., and L. D. Travis (1974), Light scattering in planetary atmosphere, *Space Sci. Rev.*, **16**, 527–610.
- Houghton, J. T., G. J. Jenkins, and J. J. Ephraums (1990), *Climate Change: The IPCC Scientific Assessment*, 365 pp., Cambridge Univ. Press, New York.
- Houghton, J. T., B. A. Callander, and S. K. Varney (1992), *Climate Change 1992: The Supplementary Report to the IPCC Scientific Assessment*, 200 pp., Cambridge Univ. Press, New York.
- Li, S., and X. Zhou (2004), Modeling and measuring spectral bidirectional reflectance factor (BRF) of snow-covered sea ice: An intercomparison study, *Hydrol. Process.*, **18**(18), 3559–3581.
- Li, S., X. Zhou, and K. Morris (1999), Measurement of snow and sea ice surface temperature and emissivity in the Ross Sea, in *IGARSS'99, IEEE 1999 International Geoscience and Remote Sensing Symposium*, vol. 2, pp. 1034–1036, Inst. of Electri. and Electron. Eng., Hamburg, Germany, 28 June–2 July.
- Liou, K.-N. (1980), *An Introduction to Atmospheric Radiation*, Elsevier, New York.
- Male, D. H., and R. J. Granger (1981), Snow surface energy exchange, *Water Resour. Res.*, **17**, 609–627.
- Marshall, S., R. J. Oglesby, K. A. Maasch, and G. T. Bates (1999), Improving climate model representations of snow hydrology, *Environ. Modelling Software*, **14**(4), 327–334.
- Massom, R. A., V. I. Lytle, A. P. Worby, and I. Allison (1998), Winter snow cover variability on East Antarctic sea ice, *J. Geophys. Res.*, **103**, 24,837–24,855.
- Massom, R. A., et al. (2001), Snow on Antarctic sea ice, *Rev. Geophys.*, **39**, 413–445.
- Morris, K., and M. O. Jeffries (2001), Seasonal contrasts in snow cover characteristics on Ross Sea ice floes, *Ann. Glaciol.*, **33**, 61–68.
- Neshyba, S. P., T. C. Grenfell, and S. G. Warren (2003), Representation of a non-spherical ice particle by a collection of independent spheres for scattering and absorption of radiation: 2. Hexagonal columns and plates, *J. Geophys. Res.*, **108**(D15), 4448, doi:10.1029/2002JD003302.
- Pearson, E. S., and H. O. Hartley (Eds.) (1966), *Biometrika Tables for Statisticians, Vol. 1*, 3rd edition, Cambridge Univ. Press, New York.
- Perovich, D. K., T. C. Grenfell, B. Light, and P. V. Hobbs (2002), Seasonal evolution of the albedo of multiyear Arctic sea ice, *J. Geophys. Res.*, **107**(C10), 8044, doi:10.1029/2000JC000438.
- Schaaf, C. B., et al. (2002), First operational BRDF, albedo and nadir reflectance products from MODIS, *Remote Sens. Environ.*, **83**(1–2), 135–148.
- Schramm, J. L., M. M. Holland, J. A. Curry, and E. E. Ebert (1997), Modeling the thermodynamics of a sea ice thickness distribution: 1. Sensitivity to ice thickness resolution, *J. Geophys. Res.*, **102**(C10), 23,079–23,092.
- Sturm, M., K. Morris, and R. Massom (1998), The winter snow cover of the West Antarctic pack ice: Its spatial and temporal variability, in *Antarctic Sea Ice: Physical Processes, Interactions and Variability*, *Antarct. Res. Ser.*, vol. 74, edited by M. O. Jeffries, pp.1–18, AGU, Washington, D. C.
- Takata, K., S. Emori, and T. Watanabe (2003), Development of the minimal advanced treatments of surface interaction and runoff, *Glob. Planet. Change*, **38**(1–2), 209–222.
- Warren, S. G. (1982), Optical properties of snow, *Rev. Geophys.*, **20**, 67–89.
- Warren, S. G., and W. J. Wiscombe (1980), A model for the spectral albedo of snow. II: Snow containing atmospheric aerosols, *J. Atmos. Sci.*, **37**, 2734–2745.
- Warren, S. G., C. J. Hahn, J. London, R. M. Chervin, and R. L. Jenne (1988), Global distribution of total cloud cover and cloud type amounts over the ocean, *NCAR Tech. Notes NCAR/TN-317+STR and DOE Tech. Rep. no. DOE/ER-0406*, U.S. Dep. of Energy, Carbon Dioxide Res. Div., Washington, D.C.
- Williams, F. (1992), *Reasoning with Statistics: How to Read Quantitative Research*, Harcourt Brace Jovanovich, Fort Worth, Tex.
- Wiscombe, W. J., and S. G. Warren (1980), A model for the spectral albedo of snow. I: Pure snow, *J. Atmos. Sci.*, **37**, 2712–2733.
- Worby, A., and I. Allison (1999), A technique for making ship-based observations of Antarctic sea ice thickness and characteristics, part I, Observational techniques and results, *Res. Rep. 14*, pp.1–23, Antarctic Coop. Res. Cent., Hobart, Tasmania, Australia.
- Worby, A., and V. Dirita (1999), A technique for making ship-based observations of Antarctic sea ice thickness and characteristics, part II, User operating manual, *Res. Rep. 14*, pp. 24–51, Antarctic Coop. Res. Cent., Hobart, Tasmania, Australia.
- Yang, Z.-L., and G.-Y. Niu (2003), The Versatile Integrator of Surface and Atmosphere processes: Part 1. Model description, *Glob. Planet. Change*, **38**(1–2), 175–189.
- Zhou, X., S. Li, and K. Stamnes (2003a), Effects of vertical inhomogeneity on snow spectral albedo and its implication for optical remote sensing of snow, *J. Geophys. Res.*, **108**(D23), 4738, doi:10.1029/2003JD003859.
- Zhou, X., S. Li, and K. Stamnes (2003b), Geometrical-optics code for computing the optical properties of large dielectric spheres, *Appl. Opt.*, **42**(21), 4295–4306.

M. O. Jeffries, S. Li, and K. Morris, Geophysical Institute, University of Alaska, P.O. Box 757320, Fairbanks, AK 99775-7320, USA. (martin.jeffries@gi.alaska.edu; sli@gi.alaska.edu; kim.morris@gi.alaska.edu)

X. Zhou, Department of Geophysical Engineering, Montana Tech of the University of Montana, 1300 West Park Street, Butte, MT 59701, USA. (xzhou@mtech.edu)